Journal of the European Ceramic Society **18** (1998) 345–351

PII: S0955-2219(97)00127-1
0955-2219/98/$19.00 + 0.00

Densification and Coarsening of SnO_2-based Materials Containing Manganese Oxide

D. Gouvea,[a]* A. Smith,[a] J. P. Bonnet[a] and J. A. Varela[b]

[a]Ecole Nationale Supérieure de Céramique Industrielle, LMCTS URA CNRS 320, 47 à 73 Avenue Albert Thomas, 87065 Limoges cedex, France
[b]Instituto de Quimica, UNESP, 14800 Araraquara, SP, Brazil

(Received 14 February 1997; accepted 16 June 1997)

Abstract

The present work presents results on natural sintering of tin dioxide ceramics, prepared by a chemical route or by conventional mixing and containing manganese ($X_{Mn} = Mn/(Mn+Sn)_{atomic}$ with $0 \leq X_{Mn} \leq 0{\cdot}15$). This cation, which is practically insoluble in SnO_2 network, stays at the grain surface. During thermal treatment ($500°C \leq T_S \leq 1400°C$), as long as the manganese surface concentration is lower than a critical value, equal to $5{\cdot}10^{-6}$ mol m^{-2}, no densification takes place. As soon as this value is reached, densification and grain growth occur simultaneously. The shrinkage kinetics is fast and high ρ/ρ_t values can be obtained (for example: $\rho/\rho_t = 0{\cdot}95$ for $T_S = 1300°C$ and $X_{Mn} = 0{\cdot}004$). The dependence between manganese content, manganese distribution, grain size and sintering behaviour is also discussed.

1 Introduction

Tin dioxide has a renewed interest due to its possible applications as a fast heating resistive element under the form of a thin layer or a dense ceramic. This later can be obtained by hot isostatic pressing (HIP)[1] or with the help of an additive like MnO_2,[2,3] CuO,[3–5] Li_2CO_3,[2] ZnO,[2,3] Nb_2O_5,[6,7] Fe_2O_3[3] or Co_2O_3.[3] If liquid phase formation can explain the influence of some of these additives on the sintering behaviour of tin dioxide (CuO or Li_2CO_3), it is not the case for most of them. The authors often assume that solid state diffusion is enhanced by the formation of defects due to the dissolution of additive derived species in the SnO_2 network.[7]

The case of manganese oxide is not clear. Its solubility, lower than 40 ppm[8] in tin dioxide lattice, implies that manganese does not affect significantly the nature and concentration of defects in bulk SnO_2. Moreover, no compound between manganese, tin and oxygen with a low melting temperature has been reported in the literature. We have shown in a previous paper that, in SnO_2 powders, manganese cations are located in a very thin *segregation* layer around the grains. If additive derived species stay at the grain periphery during the densification process, only interfacial transport properties (e.g. grain boundary diffusion) are affected by the presence of manganese atoms. Then, the additive effect depends not only on its global concentration but also on the average grain size.

The aim of the present work is to examine the sintering of tin dioxide in terms of manganese amount, grain size, porosity and additive distribution.

2 Materials

2.1 Powders

Two types of SnO_2-based powders containing manganese were prepared. The first one was obtained by a chemical route derived from Pechini's method[9] which enabled to obtain homogeneous materials in a large range of cationic ratio, X_{Mn}, ($X_{Mn} = Mn/(Mn+Sn)_{atomic}$ with $0 \leq X_{Mn} \leq 0{\cdot}15$). The procedure was the following: tin citrate was added in a mixture of citric acid and ethylene glycol. Nitric acid addition was done in order to oxidize tin (II) into tin (IV). The resulting tin (IV) citrate was soluble in the citric acid

*To whom correspondence should be addressed at: Escola Politecnica da Universidade de Sao Paulo, av. Prof. Mello Moraes, 2463 Cidade Universitaria, C.E.P. 05508-900 S. P., Brazil.

and ethylene glycol solution. The appropriate amount of manganese citrate was then added. After polymerisation between 200 and 300°C, the final resin was pyrolyzed at 400°C for 4 h and calcined at 500°C for 15 h. In some cases, further calcination treatments were also performed, for 1 h, at 500°C $\leq T_C \leq$ 900°C. The average manganese cationic ratio, X_{Mn}, controlled in the powder, was similar to its value in the initial liquid precursor.[9]

The other powder was obtained by conventional mixing of SnO_2 and MnO_2 commercial powders. Appropriate quantities (~10 g) of SnO_2 (Aldrich 99·9%) and MnO_2 (Aldrich 99%) were ball milled, for 1 h, in a nylon vessel containing dense Al_2O_3 balls and ethanol (Rhône Poulenc Normapur). Ethanol was then evaporated at 60°C for 12 h. The dried powder was fired at 400°C, for 4 h (heating and cooling ramps: 8°C min^{-1}), in order to eliminate sorbed species. After grinding in an agate mortar, the product was sifted through a 250 μm opening sieve. The specific surface area of the obtained powder, determined using BET measurements, was equal to $S_{BET} = 7{\cdot}3\ m^2\ g^{-1}$.

The powders used in the present study are identified through their origin ('*P*' for Pechini's method, '*C*' for mixing of commercial powders), manganese content, X_{Mn}, and calcination temperature. For example, a powder prepared by Pechini's method with $X_{Mn} = 0{\cdot}010$ and calcined at 500°C will be denoted '$P1{\cdot}0_{500}$'.

2.2 Ceramic preparation

Powders were uniaxially pressed (98 MPa) without any binder addition. The dimensions of the disks used for the sintering studies were 10 mm in diameter and about 2 mm thick. The dilatometric studies were performed on cylinders of 5 mm diameter and 5 mm thickness.

The first experiments indicate that manganese repartition on the grain surface is a very fast phenomenon. Therefore, to identify possible effect related to manganese inhomogeneity in *C* type powders, all sintering experiments were carried out in a furnace allowing fast firing. SnO_2-based disks supported on platinum foils were introduced in less than 10 s in the furnace previously heated at the sintering temperature ($500 \leq T_S \leq 1400$°C). When the thermo-couple located near the samples indicated that the temperature was stabilized, the corresponding time, t_S, was considered as the reference for sintering time. Stabilization of the temperature in the sample surrounding occurred in less than 30 s. After sintering (2 min $\leq t_S \leq$ 360 min), the ceramic disks and the Pt foil were air quenched. The whole process was performed in static air.

3 Ceramic characterizations

The sample densities were calculated from their mass and dimensions. Microstructural observations of dense and porous SnO_2-based ceramics were performed by scanning electron microscopy (SEM Hitachi S2500) on fracture or thermally etched surfaces. For thermal etching, carefully polished samples (with 0·3 μm alumina grains) were heated for 20 min at a temperature 50°C lower than the sintering one, T_S (heating ramp: 50°C min^{-1}).

The determination of the average grain size of those ceramics presents some difficulties. The main ones are the following:

1. chemical etching of the grain boundaries is very difficult; SnO_2 is insensitive to usual chemical reagents.
2. during thermal etching of dense materials, grain growth happened in samples previously sintered for short durations and a manganese rich phase was sometimes observed on the surface of dense samples.
3. measurements performed on micrography of etched surfaces are not reliable for ceramics of low density and small grain size due to porosity and because some grains come off during polishing.

Therefore, the average grain size reported in the following were obtained applying the linear intercept method to micrographs of fracture samples. The determination was performed using the condition described by Case *et al.*[10]

Lastly, characterization of some dense ceramics was carried out by transmission electron microscopy, TEM (Jeol FX 2010) working with a 200 kV acceleration voltage. The slices were prepared in two steps: mechanical thinning down to 40 μm followed by argon ion beam etching (acceleration voltage: 5 kV; tilt angle: 15°).

4 Influence of Manganese Content on the Sintering Behaviour

The relative densities and the microstructure of ceramics obtained after sintering, at 1300°C for 4 h, of P_{500} powders containing low manganese concentrations ($0{\cdot}000 \leq X_{Mn} \leq 0{\cdot}005$) are presented in Figs 1 and 2. Manganese addition highly promotes the densification of tin dioxide. In absence of additive, no shrinkage is observed. It can be noticed that ceramics with a density corresponding to 95% of the theoretical value, $\rho_t = 6{\cdot}95\ g\ cm^{-3}$, can be obtained for X_{Mn} as low as 0·004. Simultaneously to shrinkage, grain growth is observed.

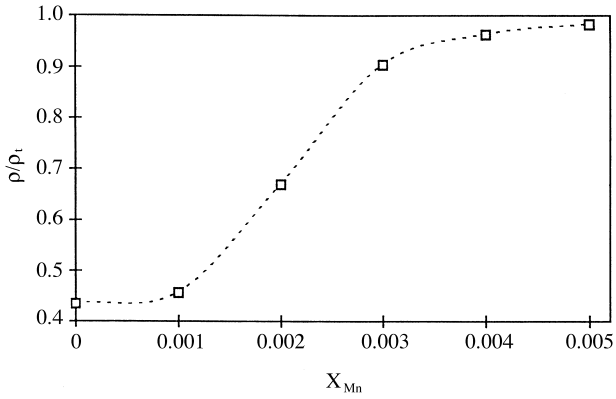

Fig. 1. Influence of X_{Mn} on the relative density (ρ/ρ_t) of ceramics sintered at 1300°C for 4 h ($\rho_t = 6{\cdot}95$ g cm^{-3}).

The evolution of the normalized density, ρ/ρ_O, versus the sintering temperature, T_S, is reported in Fig. 3 for *P* powder containing different manganese amounts ($0{\cdot}000 \leq X_{Mn} \leq 0{\cdot}060$). ρ_O and ρ correspond to the densities of green sample and ceramic heat treated for 1 h, respectively. It can be noticed that densification starts at a temperature strongly dependent on X_{Mn} The higher X_{Mn}, the lower the temperature of densification beginning.

Figure 4 shows the influence of X_{Mn} on the isothermal shrinkage of C_{400} mixtures sintered in air at 1150°C. The initial densification rate is very sensitive to X_{Mn}. In particular, the higher X_{Mn}, the faster the initial shrinkage kinetics.

The relative shrinkages observed during the dilatometric studies (dilatometer: Adamel Lhomergy DI.10.2) of $P1{\cdot}0_{500}$ and $C1{\cdot}0_{400}$ powders with identical manganese content ($X_{Mn} = 0{\cdot}010$) are reported in Fig. 5 (heating rate: 10°C h^{-1}). In both cases, shrinkage is fast. However, there is a shift towards higher temperatures for the powder prepared by conventional mixing. This temperature difference of about 100°C is observed between *P* type and *C* type powders whatever X_{Mn} is. Densification starts at lower temperature for $P1{\cdot}0_{500}$ powder for which manganese cations are homogeneously distributed *on the surface of* the tin dioxide grains prior to sintering.[11] The shift could be due to the re-distribution of the additive in the *C* powder, which would be effective from 1100°C in the experimental conditions of Fig. 5.

The variations of the ceramic average grain size, *D*, versus holding time, t_s, for $C1{\cdot}0_{400}$ samples treated at different temperatures are reported in Fig. 6(a). The higher the sintering temperature, the faster the grain growth rate. Comparison with the densification variations of the same samples [Fig. 6(b)] shows that grain coarsening and shrinkage kinetics present a similar behaviour during isothermal sintering. *P* type powders behave in the same way. Results of Figs 2 and 6 show that densification and grain growth are simultaneous phenomena.

5 Origin of Sintering in SnO_2-based Materials Containing Manganese

The fast shrinkage and the strong dependence of the densification rate on the additive amount (Fig. 4) are usual behaviour for liquid phase sintering. However, the TEM observations of a $C1{\cdot}0_{400}$ ceramic sintered at 1250°C for 20 min and quenched to room temperature did not reveal the presence of an intergranular phase. The spatial resolution of the TEM in the operating conditions was better than 1·5 Å. Moreover, grain boundaries appeared clean with SnO_2 grains in direct contact which each others as illustrated on Fig. 7. This result is in agreement with the observations of Noguès and Poix[12] who tried to prepare Mn_2SnO_4 by reaction between SnO_2 or SnO and MnO_2, Mn_2O_3 or Mn_3O_4. They never detected a liquid formation during heat treatment, even at temperature as high as 1250°C, and no reaction was observed between SnO_2 and manganese oxides.

If the observed shrinkage was related to the formation of a liquid, results reported on Fig. 3 indicate that the solidus temperature should be lower than 900°C. Therefore, there is no obvious reason to assume that the densification of SnO_2 in the presence of Mn is the result of a liquid phase sintering. The Mn presence in tin dioxide lattice was not detected in specific experiments performed on large grain ceramic.[11] The bulk Mn concentration is then lower than the detection limit of the electron microprobe, i.e. 40 ppm. The possible dissolution of such a small amount of additive cannot affect significantly the intrinsic disorder of SnO_2 at high temperature. Consequently, an improvement of volume diffusion due to Mn dissolution will not be considered in the present discussion.

In a previous paper,[11] we have reported the evolution of ρ/ρ_O versus the surface concentration of manganese, X_{Mn}/S_{PORO}, calculated assuming that all additive cations are located in an atomic layer on the grain surface. The specific surface area, S_{PORO}, of the ceramic samples was deduced from porosimetry measurements. The data showed the existence of a critical value $X_{Mn}^{SC} = 5 \times 10^{-6}$ mol m^{-2}, beyond which shrinkage begins independently of the average manganese concentration X_{Mn} (Fig. 8).

Jones and Hockey[13] have calculated that the grain surface of a rutile powder consists mainly of three families of crystallographic planes {110}, {101} and {111} in the respective percentages of 60, 20 and 20%. Assuming that Jones and Hockey crystallographic energetic considerations are valid

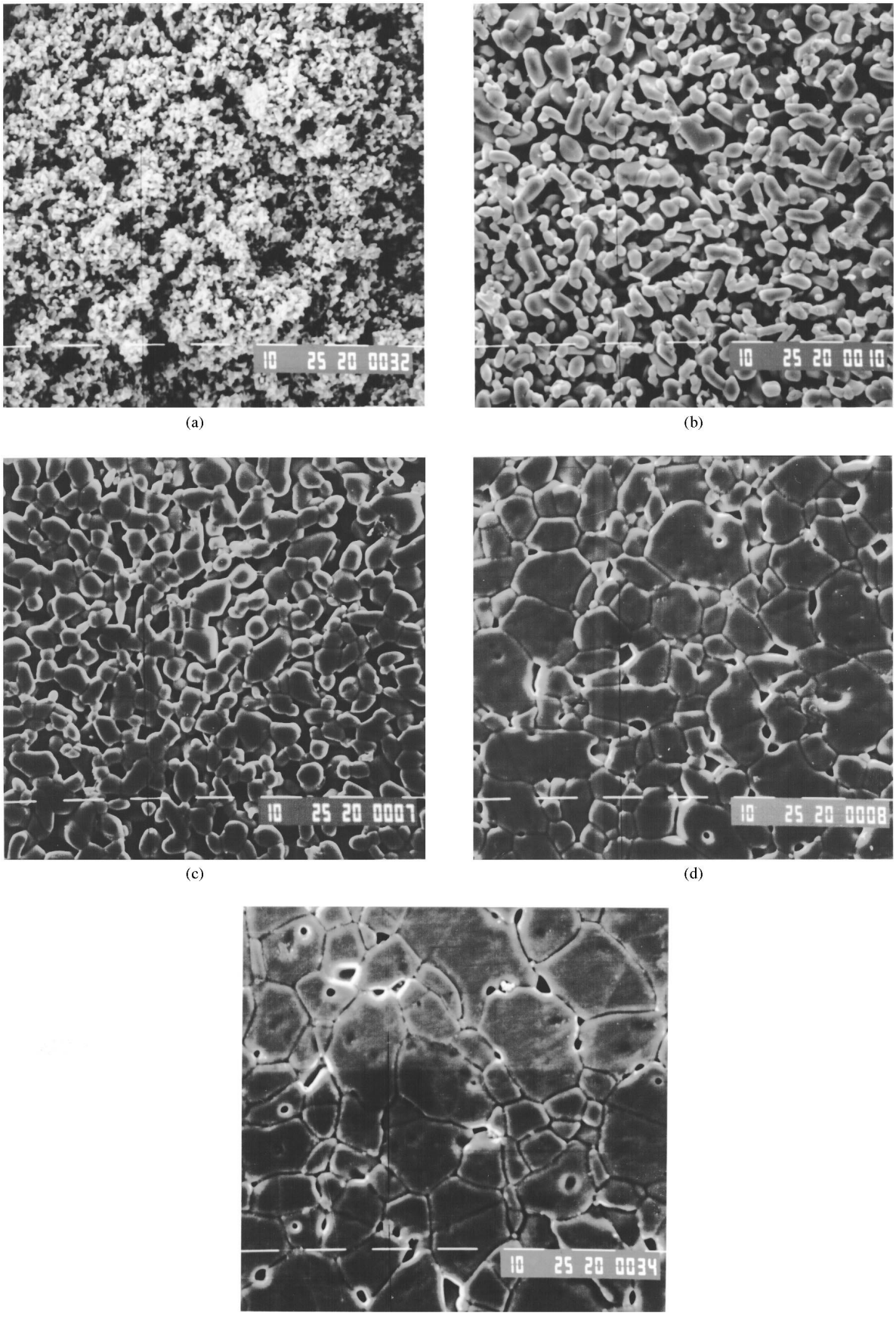

Fig. 2. Microstructures of SnO_2-based ceramics obtained by sintering P_{500} powders at 1300°C for 4 h. X_{Mn} = (a) 0·000, (b) 0·001, (c) 0·002, (d) 0·003 and (e) 0·004.

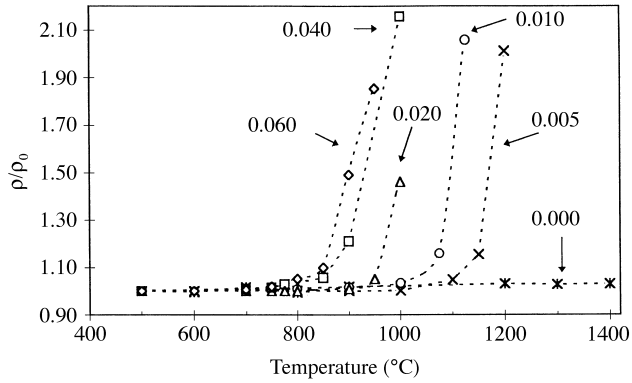

Fig. 3. Density ratio, ρ/ρ_O, versus isothermal sintering temperature, T_s, for several SnO_2-based powders prepared from Pechini's method (sintering time, t_s: 1 h; atmosphere: air).

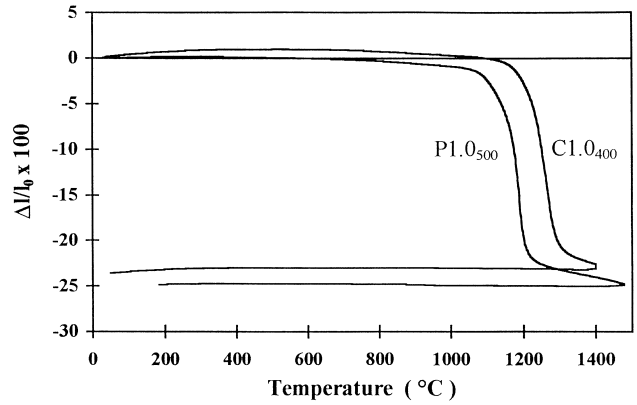

Fig. 5. Relative shrinkage versus temperature for $P1{\cdot}0_{500}$ and $C1{\cdot}0_{400}$ powders (heating ramp: 10°C min^{-1}, atmosphere: static air).

for the isotype compound SnO_2, it is possible to estimate the concentration of cationic sites occupied by tin on the grain surface. The calculation leads to $1{\cdot}41\times10^{-5}$ mol m^{-2}. This number is about three times higher than the critical concentration of Mn on the grain surface, X_{Mn}^{SC}. Therefore, we can assume that shrinkage starts when the concentration of Mn on the surface corresponds to one manganese atom for about three normal cationic sites.

The existence of a shrinkage for surface manganese concentrations greater than 5×10^{-6} mol m^{-2} suggests a change in the matter transfer regime. In other words, as long as X_{Mn}^{SC} is not reached, only the grain surface is concerned by diffusion and no densification can be observed. Beyond X_{Mn}^{SC}, the existence of a shrinkage is the signature of a new contribution to matter transport.

The most straightforward interpretation would consist to consider the promotion of grain boundary diffusion. An alternative explanation can be suggested assuming that the segregation layer affects more than one atomic plane and that its thickness is dependent on the Mn concentration on the grains. When the Mn surface concentration is larger than X_{Mn}^{SC} the thickness of the segregation layer would be large enough to envisage that the additive promotes the diffusion in a volume localized around the grains and not only on the surface.

Surface diffusion concerns oxygen vacancies, tin, oxygen and manganese species.[11] It leads to grain growth and manganese distribution. Since the solubility of manganese in SnO_2 is very low, one consequence of grain growth is an enrichment of surfaces with manganese. Shrinkage begins when the critical manganese surface concentration is reached. The temperature shift in the dilatometric curves observed in Fig. 5 can be easily understood

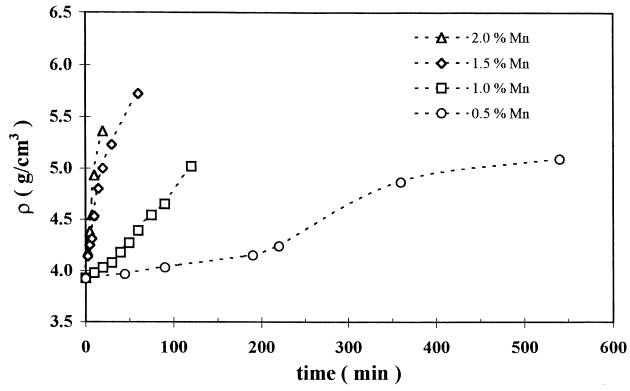

Fig. 4. Density versus holding time at 1150°C of C_{400} materials containing different X_{Mn}.

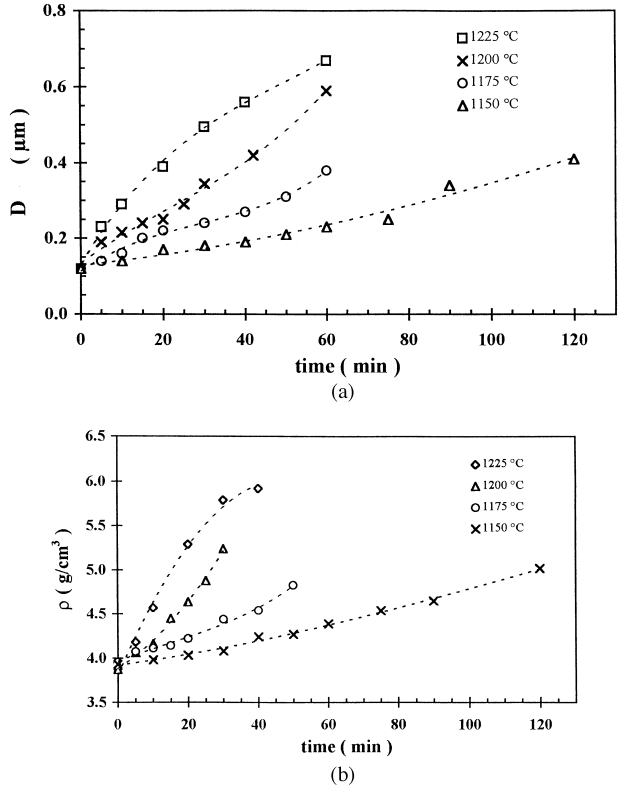

Fig. 6. Influence of holding time, t_s, on (a) average grain size, D, and (b) density, ρ, of ceramics obtained by isothermal sintering of $C1{\cdot}0_{400}$ mixtures.

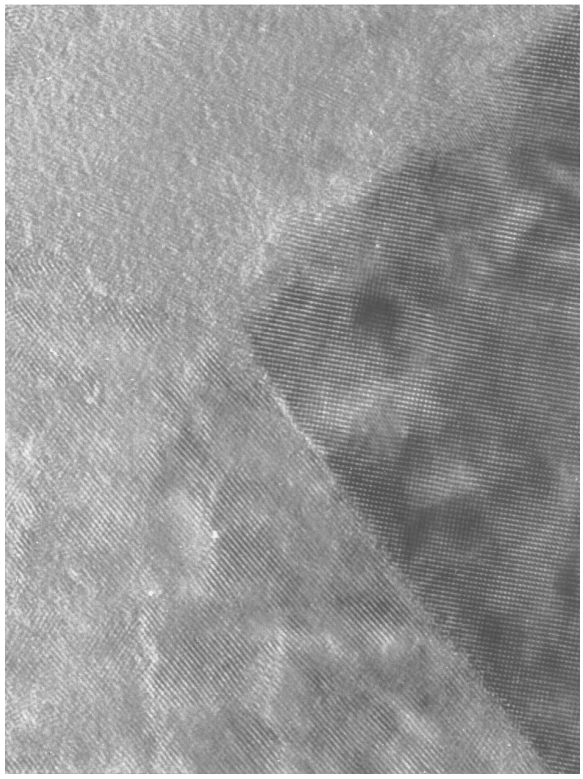

Fig. 7. Typical TEM image of a contact between three SnO_2-based grains of a $C1{\cdot}0_{400}$ ceramic sintered 20 min at 1250°C and air quenched.

if we consider that manganese is already located on the grains surfaces for *P* powders and still in manganese oxide for *C* mixtures. For inhomogeneous *C* type powder, the first effect of surface diffusion is to distribute manganese cations on the grain surface and then to increase the amount of segregated manganese; simultaneously, grains grow. Shrinkage begins later, when the X_{Mn}^{SC} value is reached. Therefore, shrinkage must begin for larger grains for *C* powder than for *P* type material. The shift towards higher temperatures observed in Fig. 5 is in agreement with such an explanation; for example, for the observed temperature of densification beginning, the grain diameter of pure SnO_2 is equal to about 180 and 300 nm, respectively.[8] The

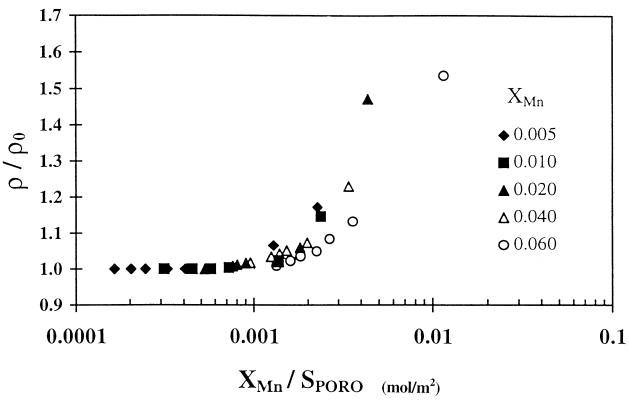

Fig. 8. Variation of ρ/ρ_O versus X_{Mn}/S_{PORO} for samples treated at different temperatures.[11]

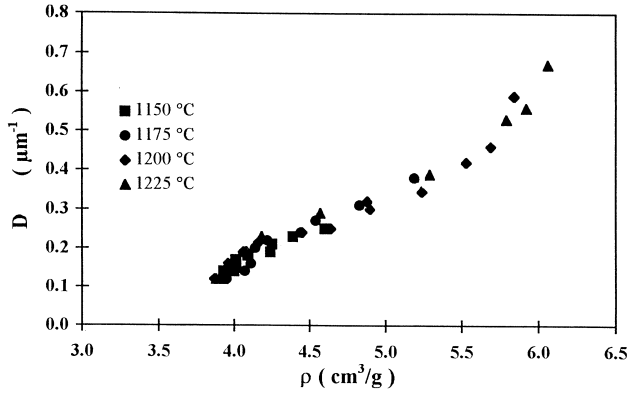

Fig. 9. Average grain size, *D*, versus sample density, ρ, for various ceramics obtained from $C1{\cdot}0_{400}$ powders sintered at different T_S.

manganese distribution during heat treatment of *C* powders can also explain why the isothermal shrinkage begins after a period which can be fairly long if X_{Mn} is low, typically 200 min at 1150°C for $X_{Mn} = 0{\cdot}005$ (Fig. 4).

6 Conclusion

Manganese cations, practically insoluble in SnO_2 network, strongly promote the densification of tin dioxide. The observed behaviours can be described by considering that the matter transport occurs only at the grain surfaces when the surface manganese concentration is lower than a critical value estimated as 5×10^{-6} mol m^{-2}. Beyond this value, densification and grain growth occur simultaneously, the shrinkage kinetics is fast and ρ/ρ_t values as high as 0·95 can be easily obtained. Higher the X_{Mn} value, lower the sintering temperature and the average grain size beyond which fast densification takes place. For example, for $X_{Mn} = 0{\cdot}004$, ceramics with closed porosity are prepared at 1300°C; for $X_{Mn} = 0{\cdot}06$, a thermal treatment at about 900°C leads to the same effect. The matter transport is no longer exclusively located at the solid/gas interface but also concerns grain boundaries or a *segregation layer around the grains*.

References

1. Park, S. J., Hirota, K. and Yamamura, H., Densification of nonadditive SnO_2 by hot isostatic pressing. *Ceram. Inter.*, 1984, **10**(3), 116.
2. Paria, M. K., Basu, S. and Paul, A., Enhanced sintering of tin dioxide with additives under isothermal conditions. *Trans Indian Ceram. Soc.*, 1983, **42**, 90–95.
3. Pennisi, L., The effect of certain oxides on the sintering and semiconducting nature of Sb_2O_3 doped SnO_2. Master thesis, Alfred University, New York, 1978.
4. Duvigneaud, P. H. and Reinhard, D., Activated sintering of tin oxide. In *Science of Ceramics*, 12, Ceramurgica s.r.l., Faenza, 1980, pp. 287–292.

5. Dolet, N., Heinz, J. M., Rabardel, L., Onillon, M. and Bonnet, J. P., Sintering mechanism of 0.99 SnO_2–0.01 CuO mixtures. *J. Mat. Sci*., 1995, **30**, 365–368.
6. Takahashi, J., Yamai, I. and Saito, H., Effect of Nb_2O_5 additive on the sintering of SnO_2. *J. Ceram. Soc. Japan*, 1975, **83**, 362.
7. Gouvea, D., Varela, J. A., Santilli, C. V. and Longo, E., Effect of niobia on the sintering of SnO_2. In *Science of Sintering—New Directions of Materials Processing and Microstructural Control*, ed. D. P. Uskokovic, H. Palmour III and R. M. Springs, Plenum Press, New York, 1989, pp. 529–536.
8. Gouvea, D., Varela, J. A., Smith, A. and Bonnet, J. P., Morphological characteristics of SnO_2 based powders containing manganese. *Eur. J. Solid State Inorg. Chem*., 1996, **33**, 343–354.
9. Gouvea, D., Varela, J. A., Longo, E., Smith, A. and Bonnet, J. P., Chemical synthesis of homogeneous SnO_2 powders doped with manganese. *Eur. J. Solid State Inorg. Chem*., 1993, **30**, 915–927.
10. Case, E. D., Smith, J. R. and Monthei, V., Grain size determinations. *Journal of the American Ceramic Society*, 1981, **2**, C24–C25.
11. Gouvea, D., Smith, A. and Bonnet, J. P., Manganese segregation on the surface of SnO_2 based powders. *Eur. J. Solid State Inor. Chem*., 1996, **33**, 1015–1023.
12. Nogues, M. and Poix, P., Contribution à l'étude de l'orthostannate de manganèse. *Ann. Chim*., 1968, **3**, 335.
13. Jones, P. and Hockey, J. A., Infra-red studies of rutile surfaces. *Trans. Faraday Soc*., 1971, **67**, 2679–2685.